CARBIDE DISTRIBUTION EFFECTS IN COLD WORK TOOL STEELS

J. Blaha, C. Krempaszky and E.A. Werner
Christian Doppler Laboratorium für Moderne Mehrphasenstähle, Lehrstuhl für Werkstoffkunde und Werkstoffmechanik, TU-München, Germany.
Postal address: Lehrstuhl für Werkstoffkunde und Werkstoffmechanik, TU-München, Boltzmannstraße 15,
85747 Garching,
Germany

W. Liebfahrt
Böhler Edelstahl GmbH & Co KG, Research & Development, Kapfenberg, Austria.
Postal address: Böhler Edelstahl GmbH & Co KG, Mariazeller Straße 25, 8605 Kapfenberg, Austria

Abstract Fracture of cold work tool steels takes place in two stages. First, microcracks are initiated at stress concentration spots like non-metallic inclusions, individual carbides and carbide clusters or (if they are present) at voids. This takes place either upon loading with stresses below the macroscopic yield or rupture strength of the material or during quenching after austenitizing. In the second stage coalescence and growth of these microcracks are observed. In this work several cold work tool steels were investigated with respect to their resistance against crack propagation, if a very sharp precrack is present. For this purpose plane strain fracture toughness tests were carried out. The resistance against crack propagation is governed mainly by the geometrical characteristics of the primary carbides (estimated in sections parallel to the fracture plane of the fractured specimens) and the mechanical properties of the constituents. Carbides are much harder than the martensitic matrix and therefore deformation is concentrated in the matrix and is impeded by the carbides. Hence, the plastic properties of the matrix are of special interest. The influence of carbides take on matrix plasticity and consequently on fracture

toughness depends mainly on their size, size distribution, volume fraction and spatial distribution.

Keywords: Cold work tool steels, fracture toughness, carbide distribution, ultra-micro indentation

INTRODUCTION

In addition to the main requirements, like high strength and wear resistance, tool steels should also possess sufficient toughness to avoid tool failure by cracking or chipping. These failure mechanisms are controlled by the propagation of intrinsic microcracks. The resistance of the material against growth of an existing crack can be measured conveniently by plane strain fracture toughness tests. Contrary to the bending rupture test, which takes into account both crack initiation and crack growth, plane strain fracture toughness tests only consider the latter. Crack growth is governed mainly by the content, size and distribution of the primary carbides and the mechanical properties of the matrix. The content of primary carbides is determined by the amount of carbon and carbide forming elements like chromium, molybdenum, vanadium, tungsten and niobium. These elements improve wear resistance and hardness of the material but impair toughness, because of their strong tendency to segregate during solidification. The production of high speed and cold work tool steels via the powder metallurgical (PM) route [1, 2, 3] provides the possibility to use higher contents of carbide forming elements, because segregation is suppressed due to a very high solidification rate (10^4 to 10^6 Ks^{-1}) during the atomization process. The resulting homogeneous microstructure consists of a martensitic matrix with embedded globular and evenly distributed primary carbides with a size in the μm range. Although the microstructure is rather homogeneous there are, depending on the composition, carbide types, production parameters and austenitizing temperature, differences in the size and the distribution of the carbides. The influence of these parameters on fracture toughness is investigated here by comparing different steels with a similar total amount of primary carbides. The mechanical properties of the matrix are characterized by "Ultra-Micro" hardness tests (UMHT) and by tensile tests, assuming that plastic deformation will start in the softer matrix and that the yield strength of the matrix is the yield strength of the compound. The coherent secondary

carbides ($\approx$ nm) precipitated during tempering are treated as a part of the matrix.

EXPERIMENTAL

Four alloys were produced via the PM route. Table 1 shows their chemical composition and the primary carbides present. In addition to the elements listed the steels contain vanadium between 2 and 4 %. All four steels possess a carbide volume fraction between 11.1 and 13.1 %. The heat treatment performed consists of austenitizing in the two or multi phase region austenite (γ) and carbide(s), followed by quenching and three times tempering to a final hardness of about 60 HRC. The whole treatment was done in liquid salt bath furnaces, because of the excellent heat transfer and the uniformity of temperature in the melt.

Table 1. Chemical composition in wt.% and carbide types of the materials investigated. M denotes carbide forming elements other than Nb

Steel	C	Si	Mn	Cr	Mo	W	Nb	Carbides
I	1.8	0.8	0.4	8	3	—	3	MC,NbC,M_7C_3
II	1.8	1.0	0.4	8	2	—	3	MC,NbC,M_7C_3
III	1.9	0.7	0.4	7	3	—	3	MC,NbC,M_7C_3
IV	1.1	0.2	0.2	4	8	0.3	0.1	MC,M_6C

Using a scanning electron microscope (SEM) and two types of image generation, the secondary-electron (SE) or the backscattered-electron (BE) mode [4], the carbides (MC, M_7C_3, M_6C) and the matrix could be differentiated (Fig. 1). Both modes can be used without prior etching of the specimen surface. The carbides vary strongly in composition, which is true especially for the monocarbide MC sometimes being rich in niobium (NbC) and appearing white (Steels I, II and III in Fig. 1 (a), (b), (d)) or rich in vanadium then appearing dark gray (Steels I, II, III and IV in Fig. 1 (a), (c), (e), (f)). This varying composition causes difficulties in distinguishing between MC and M_7C_3 carbides.

Quantitative microstructure analysis was performed on sections parallel to the fracture surface of single edge notched 3-point bending (SENB)

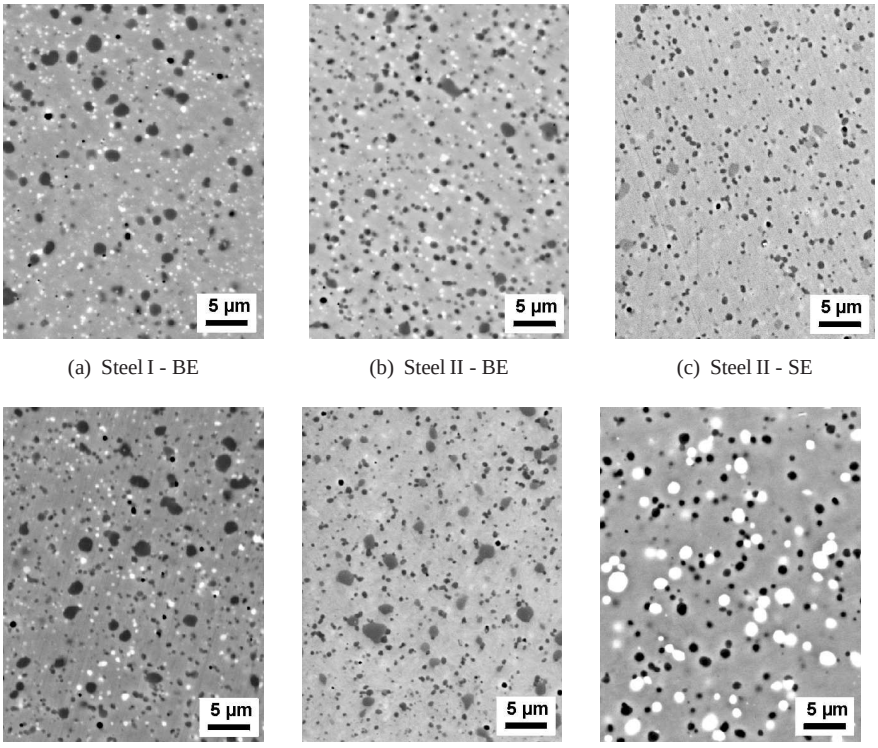

(a) Steel I - BE (b) Steel II - BE (c) Steel II - SE

(d) Steel III - BE (e) Steel III - SE (f) Steel IV - BE

Figure 1. Scanning electron micrographs of the microstructure of the materials investigated. BE = backscattered electron mode, SE = secondary electron mode.

specimens. These specimens of dimensions $12 \times 6 \times 60$ (W×B×L, all in mm) were taken from hot rolled bars (∅ = 32 mm and 43 mm) and were subjected to the measurement of the plane strain fracture toughness according to ASTM E399-90 [5]. The precrack consisted of a milled notch, deepened by electroerosive machining and a fatigue crack of about ≈100 µm length, which was introduced by compressive cyclic loading (Fig. 2 (a)). Then the precracked specimens were loaded to failure (Fig. 2 (b)). Since the load-displacement curves did not show any signs of plastic deformation (Fig. 2 (c)), the maximum load P_{Q} could be used to calculate the value K_{Q}, which corresponds to K_{IC}, if some validity requirements are fulfilled [5].

To ensure plane strain conditions the dimensions of the specimen have to be taken sufficiently large and the crack tip plastic region must be small compared to both the crack length and the specimen dimensions.

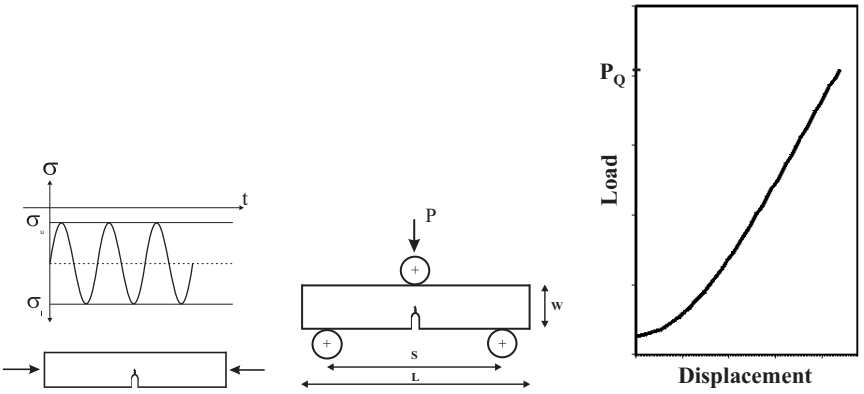

(a) Compressive cycling loading. (b) 3-point bending fixture. (c) Load-Displacement curve.

Figure 2. Plane strain fracture toughness testing.

The yield strength σ_{YS} was estimated from uniaxial tensile tests and allows, together with K_{IC}, to calculate the size of the plastic zone in front of the crack tip, r_{P}, from [6, 7, 8, 9]:

$$r_{\mathrm{P}} = \frac{1}{6\pi}\left(\frac{K_{\mathrm{IC}}}{\sigma_{\mathrm{YS}}}\right)^2 \tag{1}$$

Although our materials are very hard, all four steels show noticeable plastic deformation in the tensile tests. The in-situ hardness of the matrix material is characterized by indentation tests with an "Ultra-Micro" indenter mounted in a scanning electron microscope. Using always the same indentation force (19.9 mN) and the same indentation time (15 s) makes possible to compare the hardness of the matrices of the four steels by comparing the length of the indentation diagonals. From these tests the relative matrix hardness is characterized by the value $d_{\min}/d$ (Table 2), where $d_{\min}$ is the smallest indentation diagonal observed in the steel with the hardest matrix (steel I). Hence, the higher the value $d_{\min}/d$, the harder is the in-situ hardness of the matrix.

RESULTS AND DISCUSSION

Figure 3 (a) shows the size distribution of all particles (primary carbides and non-metallic inclusions, NMI) present in the steels. The measured values are approximated by logarithmic normal distributions. For the sake of clarity the measured values are only displayed in (Fig. 3 (b)) by symbols, where for steel III carbides and non-metallic inclusions are separated. M_7C_3 and MC are treated as one particle type due to the difficulties to distinguish them properly with the image analysis system. For macroscopic properties like hardness, fracture toughness or tensile strength the type of carbide is not so important, since irrespective of their chemical composition carbides are always much harder than the matrix and are not deformed plastically.

Particles of type M_7C_3, which appear light gray (Fig. 1 (e)), are larger than MC (dark gray). Their number is low with a size of at least 1 µm. In Table 2 the mechanical properties and the microstructural parameters are listed. The total volume fraction of particles (carbides and NMI) varies not very much, compared to carbide contents of commercial PM tool steels between 5 and 30 %.

Table 2. Rockwell hardness, plane strain fracture toughness, volume fraction of particles (carbides and NMI), mean particle diameter, mean interparticle spacing λ [10], size of the plastic zone r_p, difference $\lambda - r_\mathrm{p}$ and relative hardness of the martensitic matrix d_min/d of the investigated steels.

Steels	I	II	III	IV
Hardness [HRC]	59.8	59.4	59.2	60.4
K_IC [MPa $\sqrt{\mathrm{m}}$]	17.7	16.4	14.9	18.7
volume fraction of particles [%]	11.1	12.0	12.7	13.1
mean particle diameter [µm]	0.51	0.45	0.46	0.74
λ [µm]	4.08	3.32	3.31	4.91
r_p [µm]	2.74	2.56	2.11	3.14
λ - r_p [µm]	1.34	0.76	1.20	1.77
d_min/d	1	0.94	0.96	0.87

Steel IV shows the highest fracture toughness (Table 2) even though it possesses the highest macrohardness and the largest mean particle size. While an increase of these properties is usually associated with a reduction in tough-

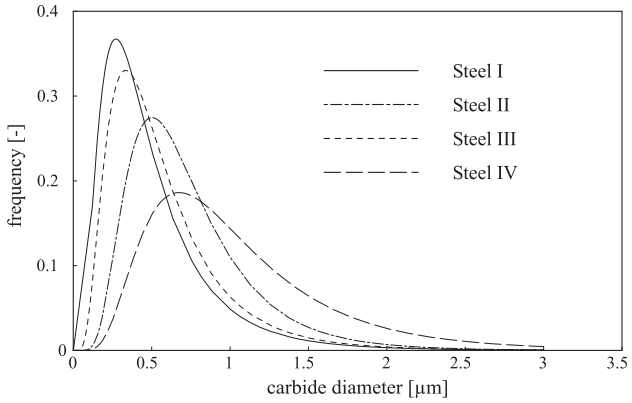

(a) Particle size distribution of the investigated steels.

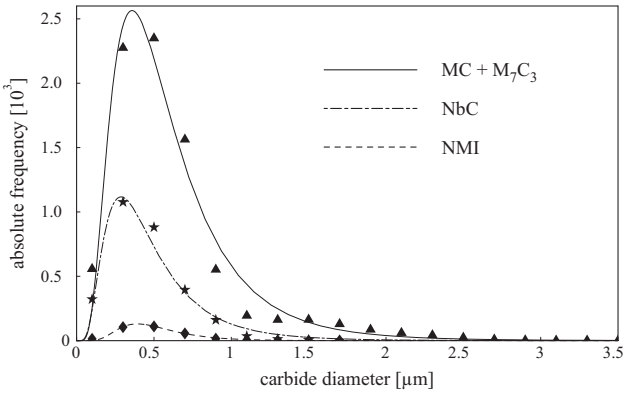

(b) Size distribution of the particle types in steel III. The symbols represent measured values.

Figure 3. Particle size distributions approximated by the logarithmic normal distribution.

ness, one has to keep in mind that this steel possesses the softest matrix and the largest interparticle spacing, which both increase toughness. Analyzing the fracture surfaces of the tensile specimens shows that even the largest single carbide is not large enough to act as a critical flaw, and hence carbide clusters, non-metallic inclusions, voids or impurities act as crack initiating flaws. Increasing the size of the particles rather improves the resistance

against crack growth in the investigated steels since for a given carbide content larger particles result in larger distances between the carbides.

Hard inclusions and the inclusion/matrix interface possess a lower resistance against crack propagation than the martensitic matrix, which dissipates a part of the energy released during fracture by plastic deformation. However, a crack can interact with a carbide only, if the carbide is within the plastic zone around the crack tip [11]. Antretter et al. [12] investigated an arrangement of two brittle inclusions in a ductile matrix by means of finite element calculations and found that in the case of two undamaged particles small interparticle distances reduce the risk of particle failure due to stress relaxation on either side of the particles. If, however, one of the particles is already broken, the stress concentration around the crack tip increases the stress inside the other inclusion as the crack approaches the interface between the matrix and this second particle. Therefore, a large distance between the particles decreases the sensitivity to failure, so increasing K_{IC}. The interaction of a crack and the nearest carbide in the direction of crack growth depends mainly on the distance between the carbides and the deformation behaviour of the matrix [13]. Figure 4 shows the fracture toughness as a function of the mean interparticle distance. Even though the graph stipulates that K_{IC} should always be large if λ increases, one has to keep in mind also the deformation properties of the matrix. These can be estimated roughly by calculating the size of the plastic zone, r_{p}, in front of the crack tip (Equation 1). Within the experimental scatter one can conclude that a large difference between the mean interparticle spacing and the calculated size of the plastic zone ($\lambda - r_{\mathrm{p}}$) seems to be beneficial for the plane strain fracture toughness of this high strength material class (Table 2).

Ultra-micro hardness and the yield strength both describe the plastic deformation behaviour of the matrix. While the yield strength, estimated in uniaxial tensile tests, characterizes the onset of plastic deformation in the compound matrix/primary carbide and is almost the same in all four steels ($\sigma_{\mathrm{YS}} = 2400 \pm 50$ MPa), ultra-micro hardness is a quantity characterizing the flow behaviour of the matrix and shows distinct differences. This can be explained by the different tempering states of the matrices. For the same macroscopic hardness the special composition of the steels, and consequently tempering behaviour, results in different amounts and sizes of the secondary carbides, which affect the plastic deformation behaviour of the matrix (martensite + secondary carbides). The second reason is the different

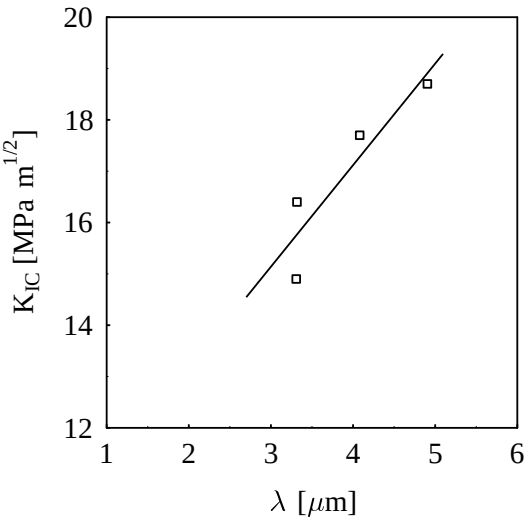

Figure 4. Plane strain fracture toughness K_{IC} vs. mean interparticle spacing λ.

primary carbide spacing. Assuming that the dimension of the stressed volume affected by the ultra-micro indentation is at least several µm, then this volume will most probably interact with one or more primary carbides. The contribution of the primary carbides to this hardness measure is the stronger the smaller the interparticle spacing is.

The results presented clearly show that cold work tool steels produced via the PM route possess distinctly different fracture toughness K_{IC} even though the steels investigated contain roughly the same particle volume fraction and are adjusted to the same macroscopic hardness. A fine distribution is desirable in order to delay crack initiation, but small interparticle distances decrease the resistance of the material against crack propagation. Hence, K_{IC} is closely related to the mean interparticle spacing λ and the size of the plastic zone r_{p} and, therefore, to the yield strength of the martensitic matrix.

REFERENCES

[1] W. SCHATT and K.-P. WIETERS: Pulvermetallurgie - Technologien und Werkstoffe. VDI Verlag, Düsseldorf (1994).

[2] A. KASAK and E. J. DULIS: Powder-metallurgy tool steels. Powder Metallurgy, 21 (1978) 114–121.

[3] P. HELLMANN: High speed steels by powder metallurgy. Veitsch-Radex Rundschau, 1 (1999) 16–29.

[4] E. BISCHOFF and H. OPIELKA, I. KABYEMERA and S. KARAGÖZ: REM-Untersuchungen zur quantitativen Metallographie von Karbiden in Schnellarbeitsstählen. Prakt. Metallographie, 32 (1995) 77–89.

[5] ASTM Standard E399-90 (Reapproved 1997): Standard Test Method for Plane-Strain Fracture Toughness of Metallic Materials, volume 3.01. Philadelphia, PA: American Society for Testing and Materials (1997).

[6] R. O. RITCHIE and J. F. KNOTT: On the relationship between critical tensile stress and fracture toughness in mild steel. J. Mech. Phys. Solids, 21 (1973) 395–410.

[7] M. A. GOMES, A. S. WRONSKI and C. S. WRIGHT: Fracture behaviour of highly alloyed high speed steel. Fatigue and Fracture of Engineering Materials and Structures, 18 (1995) 1–18.

[8] D. F. WATT, P. NADIN and S. B. BINER: The fracture toughness of hardened tool steels. J. Engineering Materials and Technology, 109 (1987) 314–318.

[9] L. R. OLSSON and H. F. FISCHMEISTER: Fracture toughness of powder metallurgy and conventionally produced high speed steels. Powder metallurgy, 21 (1978) 13–28.

[10] G. E. PELLISSIER and S. M. PURDY: Stereology and quantitative metallography STP 504. Philadelphia, PA: American Society for Testing and Materials (1972).

[11] H. FISCHMEISTER and L.R. OLSSON: Fracture toughness and rupture strength of high speed steels. Cutting Tool Materials (1981) 111–132.

[12] T. ANTRETTER and F. D. FISCHER: Particle cleavage and ductile crack growth in a two-phase composite on a microscale. Computational Materials Science, 13 (1998) 1–7.

[13] J. BLAHA, E. A. WERNER and W. LIEBFAHRT: The influence of the microstructure on the fracture toughness of cold work tool steels. In: Proc. of the European Congress and Exhibition on Powder Metallurgy, 22nd–24th October 2001, Nice, F, European Powder Metallurgy Association (2001) 73–78.